Письма в ЭЧАЯ. 2014. Т. 11, № 4(188). С. 568–581

EVOLUTION OF THE TRUNCATED MELLIN MOMENTS OF THE PARTON DISTRIBUTIONS IN QCD ANALYSIS

D. Kotlorz [a,1], *A. Kotlorz* [b,2]

[a] Opole University of Technology, Division of Physics, Opole, Poland

[b] Opole University of Technology, Division of Mathematics and Applied Informatics, Opole, Poland

We review evolution equations for the truncated Mellin moments of the parton distributions and some their applications in QCD analysis. The main finding of the presented approach is that the nth truncated moment of the parton distribution obeys also the DGLAP equation but with a rescaled splitting function $P'(z) = z^n P(z)$. This allows one to avoid the problem of dealing with the experimentally unexplored Bjorken-x region. The evolution equations for truncated moments are universal — they are valid in each order of perturbation expansion and can be a useful additional tool in analysis of unpolarized as well as polarized nucleon structure functions.

Рассматриваются уравнения эволюции усеченных моментов Меллина партонных распределений и некоторые их приложения в КХД-анализе. Основным результатом проделанной работы является вывод, что n-й усеченный момент подчиняется также уравнению DGLAP, но с перемасштабированной функцией расщепления $P'(z) = z^n P(z)$. Такой подход позволяет избежать необходимости работать в экспериментально не исследованной области значений бьеркеновской переменной x. Уравнения эволюции для усеченных моментов являются универсальными: их можно использовать в любом порядке разложения в ряд теории возмущений, и они могут оказаться полезным дополнительным инструментом в анализе как неполяризованных, так и поляризованных структурных функций.

PACS: 12.38.Bx; 11.55.Hx

INTRODUCTION

Understanding the details of the Bjorken-x and Q^2 dependence of the nucleon structure functions is one of the most important challenges in high-energy physics. Perturbative QCD provides a comprehensive framework for describing deep-inelastic lepton–hadron scattering (DIS) and hadron–hadron collisions (H–H) in current and planned experiments. In this framework, where the high-energy collisions proceed via partonic constituents of the hadron, a key role is played by universal parton distribution functions (PDFs). According to the factorization theorem, DIS or H–H cross section is a convolution of a short-distance interaction,

[1] E-mail: d.strozik-kotlorz@po.opole.pl

[2] E-mail: a.kotlorz@po.opole.pl

described by the partonic cross section $\hat{\sigma}_f$ and a long-distance structure described by the parton distribution q_f.

Particularly interesting is a study of polarized processes which provides knowledge of the spin structure of the nucleon. Though the recent experimental data and NLO analyses suggest that valence quarks carry the expected fraction of the nucleon spin, the main questions are still open: how the nucleon spin is distributed among its constituents — quarks (particularly sea quarks with negative helicity) and gluons, and how the dynamics of these constituent interactions depends on spin. New experimental data in the resonance region from Jefferson Lab together with complementary data from HERMES, COMPASS and RHIC, are a crucial step towards better understanding of not only the flavor decomposition and gluon contributions to the nucleon spin but also the quark–hadron duality. The main goal of present polarized experiments is to determine the nucleon spin structure functions $g_1(x, Q^2)$, $g_2(x, Q^2)$ and their moments which are essential in testing QCD sum rules. The theoretical approach usually used in the description of these experimental results is the QCD evolution equations for the parton densities which change with Q^2 according to the well-known DGLAP equations [1–4]. This standard DGLAP approach operates on the parton densities q; hence their moments, which are, e.g., the contributions to the proton spin and other sum rules, can be obtained by the integration of the parton densities q over Bjorken-x.

Alternatively, one can directly study the Q^2 evolution of the Mellin moments of the parton densities. The moments provide a natural framework in QCD analysis, as they originate from OPE — the basic formalism of quantum field theory. The idea of truncated Mellin moments (TMM) of the parton densities in QCD analysis was introduced and developed in the late 1990s [5–8]. The authors obtained the nondiagonal differential evolution equations in which the nth truncated moment coupled to all higher ones. The evolution equations for TMM within the $\ln^2 x$ approximation were found in [9], and finally DGLAP-type diagonal integro-differential evolution equations for the single- and double-truncated moments of the parton distribution functions were derived in [10, 11] and [12]. Evolution equations for double-truncated moments and their application to study the quark–hadron duality were also discussed in [13].

The main finding of the truncated moments approach is that the nth moment of the parton distribution obeys also the DGLAP equation but with a rescaled splitting function $P'(z) = z^n P(z)$ [10]. This approach allows one to restrict the analysis to the experimentally available Bjorken-x region. The evolution equations for TMM are universal — they are valid in each order of perturbation expansion (then Wilson coefficients rescale in the same way as the splitting functions) and can be an additional tool in QCD analysis of unpolarized as well as polarized nucleon structure functions.

In this paper, we review our main results on the truncated moments approach. In the next section, we present the evolution equations for the truncated moments of the parton distributions. Section 2 contains relations between the truncated and untruncated Mellin moments, useful for solving evolution equations. Section 3 describes determination of the parton densities from their truncated moments. Implications of the TMM approach for analysis of the polarized structure functions g_1 and g_2 are presented in Secs. 4 and 5, respectively. We show the evolution of TMM of g_1 together with the predictions for the Bjorken sum rule. Then, we present the Wandzura–Wilczek relation and sum rules in terms of the truncated moments. We also give the evolution equations. Finally, in Summary, we highlight possible future applications of the truncated moments approach in QCD analysis.

1. THE EVOLUTION EQUATIONS FOR THE TRUNCATED MELLIN MOMENTS OF THE PARTON DISTRIBUTIONS

The structure functions of the nucleon can be expressed in terms of the parton distributions. These depend on two kinematic variables: the Bjorken-x and $Q^2 = -q^2$ with q being the four-momentum transfer in the deep-inelastic lepton–nucleon scattering (DIS). The scaling variable is defined as $x = Q^2/(2pq)$, where p is the nucleon four-momentum. The strong interactions between quarks and gluons cause changes in the parton densities. For medium and large x, the Q^2 evolution of the parton distributions is described by the standard Dokshitzer–Gribov–Lipatov–Altarelli–Parisi (DGLAP) equations [1–4]:

$$\frac{dq(x,Q^2)}{d\ln Q^2} = \frac{\alpha_s(Q^2)}{2\pi}\,(P\otimes q)(x,Q^2), \tag{1}$$

where $\alpha_s(Q^2)$ is the running coupling, $\otimes$ denotes the Mellin convolution

$$(A\otimes B)(x) \equiv \int\limits_x^1 \frac{dz}{z}\,A\left(\frac{x}{z}\right)\,B(z), \tag{2}$$

and $P(z)$ is the splitting function, which can be expanded in a power series of $\alpha_s(Q^2)$.

In the DGLAP approach, the main role is played by the PDFs and in our TMM approach we study directly the Q^2 evolution of the truncated moments of the PDFs. In [10], we found that the single-truncated moments of the parton distributions $q(x,Q^2)$, defined as

$$\bar{q}^n(x_0,Q^2) = \int\limits_{x_0}^1 dx\,x^{n-1}\,q(x,Q^2), \tag{3}$$

obey the DGLAP-type equation

$$\frac{d\bar{q}^n(x_0,Q^2)}{d\ln Q^2} = \frac{\alpha_s(Q^2)}{2\pi}\,(P'\otimes\bar{q}^n)(x_0,Q^2). \tag{4}$$

A role of the splitting function is played here by $P'(n,z)$:

$$P'(n,z) = z^n\,P(z). \tag{5}$$

Since the experimental data cover only a limited range of x, except very small $x\to 0$ as well as large $x\to 1$, it is very natural and convenient to deal with the double-truncated moments. Truncation at large x is less important in comparison to the small-x limit because of the rapid decrease of the parton densities as $x\to 1$; nevertheless, a comprehensive theoretical analysis requires an equal treatment of both truncated limits.

The double-truncated moment

$$\bar{q}^n(x_{\min},x_{\max},Q^2) = \int\limits_{x_{\min}}^{x_{\max}} dx\,x^{n-1}\,q(x,Q^2), \tag{6}$$

as it is a subtraction of two single-truncated ones, also satisfies the DGLAP-type evolution equation (4) [11–13]:

$$\frac{d\bar{q}^n(x_{\min}, x_{\max}, Q^2)}{d\ln Q^2} = \frac{\alpha_s(Q^2)}{2\pi} \int\limits_{x_{\min}}^{1} \frac{dz}{z}\, P'(n,z)\, \bar{q}^n\left(\frac{x_{\min}}{z}, \frac{x_{\max}}{z}, Q^2\right) \tag{7}$$

with P' given again by Eq. (5).

Our approach, Eqs. (4)–(7), is valid for the coupled DGLAP equations for quarks and gluons and for any approximation (LO, NLO, NNLO, etc.). For clarity, we present here only the nonsinglet and leading order part. In higher order analysis (e.g., NLO), truncated moments of the structure functions assume the form

$$\bar{g}_1^n(x,Q^2) = \frac{1}{2}\sum_q e_q^2 \times \\ \times \left[\Delta\bar{q}^n(x,Q^2) + \frac{\alpha_s(Q^2)}{2\pi}\left(C'_q(n) \otimes \Delta\bar{q}^n + C'_G(n) \otimes \Delta\bar{G}_n\right)(x,Q^2)\right], \tag{8}$$

where the Wilson coefficients rescale in the same way as the splitting functions

$$C'_i(n,x) = x^n\, C_i(x). \tag{9}$$

Let us emphasize that the evolution equations for the double-truncated moments, Eq. (7), are in fact a valuable generalization of those for the single-truncated and untruncated ones. Setting $x_{\min} = x_0$ or $x_{\min} = 0$ and $x_{\max} = 1$, one obtains Eq. (4) or the well-known renorm-group equation for the moments

$$\frac{d\bar{q}^n(Q^2)}{d\ln Q^2} = \frac{\alpha_s(Q^2)}{2\pi}\, \gamma^n(Q^2)\, \bar{q}^n(Q^2), \tag{10}$$

respectively.

In the next section, we present relations between truncated and untruncated moments which are useful for solving the evolution equations.

2. RELATIONS BETWEEN TRUNCATED AND UNTRUNCATED MOMENTS

The evolution equations for the truncated moments, Eq. (4), are very similar to those for the PDFs. In both cases, one deals with functions of two variables x and Q^2 (with additionally fixed index n for moments), which obey the integro-differential Volterra-like equations. The only difference lies in the splitting function, which for moments has the rescaled form Eq. (5). This similarity allows one to solve the equations for truncated moments with the use of standard methods of solving the DGLAP equations. Analysis of the evolution performed in moment space, when applied to the truncated moments, implies dealing with such an exotic structure as «Moment of Moment». Let us discuss this in detail and introduce some useful relations involving untruncated and truncated Mellin moments.

There are in literature several methods for the solution of the integro-differential DGLAP equations. They are based on either the polynomial expansion or the Mellin transformation —

for review see, e.g., [14]. In our previous studies on the evolution of the truncated moments we used the Chebyshev polynomial technique [15], earlier widely applied by Jan Kwieciński in many QCD treatments — for details see, e.g., Appendix of [16]. Using this method, one obtains the system of linear differential equations instead of the original integro-differential ones. The Chebyshev expansion provides a robust method of discretising a continuous problem.

An alternative approach is based on the Mellin transformation and the moment factorization. Taking the sth moment of the evolution equation (4), one obtains

$$\frac{dM^{s,\,n}(Q^2)}{d\ln Q^2} = \frac{\alpha_s(Q^2)}{2\pi}\,\gamma^{s+n}(Q^2)\,M^{s,\,n}(Q^2), \tag{11}$$

where $M^{s,\,n}$ denotes here the sth (untruncated) moment of the nth (truncated) moment of the parton density

$$M^{s,\,n}(Q^2) = \int\limits_0^1 dx\,x^{s-1}\,\bar{q}^n(x,Q^2). \tag{12}$$

Analogically to the well-known solutions for the PDFs, we can immediately write down solutions for the truncated moments

$$M^{s,\,n}(Q^2) = M^{s,\,n}(Q_0^2)\left[\frac{\alpha_s(Q_0^2)}{\alpha_s(Q^2)}\right]^{b\,\gamma^{s+n}} \tag{13}$$

and

$$\bar{q}^n(x,Q^2) = \frac{1}{2\pi i}\int\limits_{c-i\infty}^{c+i\infty} ds\,x^{-s}\,M^{s,\,n}(Q^2). \tag{14}$$

The quantity $M^{s,\,n}$, which is rather exotic and has no physical meaning, can be replaced by the usual truncated moment $\bar{q}$. In [12], we found useful relations between the truncated and untruncated moments, namely,

$$M^{s,\,n} = \frac{1}{s}\int\limits_0^1 dz\,z^{s+n-1}q(z) = \frac{1}{s}\,\bar{q}^{s+n}, \tag{15}$$

$$\bar{q}^n(x,Q^2) = \frac{1}{2\pi i}\int\limits_{c-i\infty}^{c+i\infty} ds\,\frac{x^{-s}}{s}\,\bar{q}^{s+n}(Q^2) \tag{16}$$

and

$$\bar{q}^s(Q^2) = (s-n)\,M^{s-n,\,n}(Q^2) = (s-n)\int\limits_0^1 dx\,x^{s-n-1}\,\bar{q}^n(x,Q^2). \tag{17}$$

Equations (15), (16) and (17) have a large practical meaning in solving the evolution equations of TMM. Particularly, Eq. (16) seems to be helpful when the untruncated moments are known, e.g., from lattice calculations.

In the next sections we will discuss some implications of our approach for QCD analysis.

3. DETERMINATION OF THE PARTON DISTRIBUTIONS FROM THEIR TMM

The TMM approach, which refers to the physical values — moments (not to the parton densities), allows one to study directly their evolution and the scaling violation. The solutions for truncated moments can also be used in the determination of the parton distribution functions via differentiation

$$q(x,Q^2) = -x^{1-n}\,\frac{\partial \bar{q}^n(x,Q^2)}{\partial x}. \tag{18}$$

In order to reconstruct initial parton densities at scale Q_0^2 from their truncated moments, given, e.g., by experimental data at scale Q^2, we evolve moments between these two scales down (from Q^2 to Q_0^2) and then perform the final fit of free parameters — for details see [11].

We proceed with the following steps:

1. Preparing available experimental data for moments $\bar{q}^n(x_0,Q_1^2)$ as a function of $x_{\min} \leqslant x_0 \leqslant 1$ at the same scale Q_1^2.

2. Interpolation of the given data points into the points that are Chebyshev nodes. This allows us to use the Chebyshev polynomial technique for solving the evolution equations.

3. Evolution of the truncated moments from Q_1^2 to Q_2^2, according to (1), for different $x_{\min} \leqslant x_0 \leqslant 1$.

4. Reconstruction of the parton density $q(x,Q_2^2)$ from its truncated moment at the same scale Q_2^2 by applying the minimizing algorithm to fit free parameters.

In [11], we tested this method on the nonsinglet function parameterized in the general form

$$q(x,Q_0^2) = N(\alpha,\beta,\gamma)\,x^{\alpha}(1-x)^{\beta}(1+\gamma x), \tag{19}$$

and also on the original fits for HERMES [17] and COMPASS [18] data. In Figs. 1 and 2, we show the spin-dependent valence quark distributions reconstructed from HERMES [17] and COMPASS [18] data. From these plots one can see satisfactory agreement between the

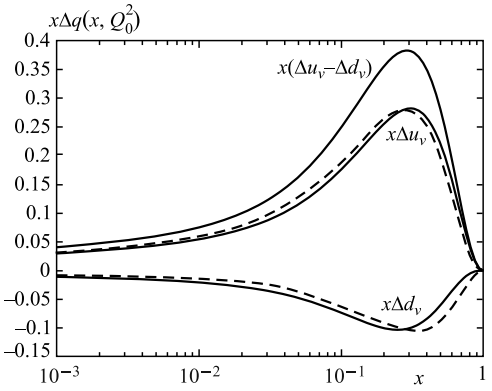

Fig. 1. Initial spin-dependent valence quark distributions $x(\Delta u_v - \Delta d_v)$, $x\Delta u_v$ and $x\Delta d_v$ at $Q_0^2 = 4$ GeV^2: dashed — reconstructed from HERMES data for the first truncated moment of the nonsinglet polarized function $g_1^{\rm NS}$ at $Q^2 = 5$ GeV^2 [17], solid — original BB fit [19]. Plots for $x(\Delta u_v - \Delta d_v)$ overlap each other

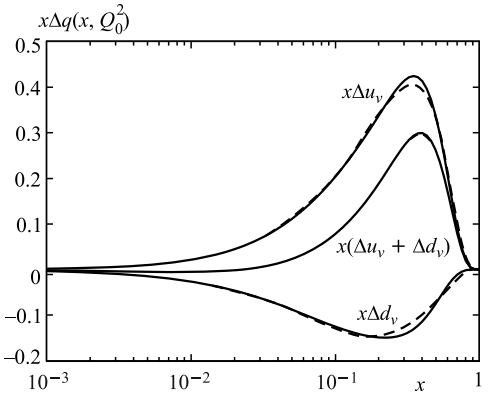

Fig. 2. Initial spin-dependent valence quark distributions $x(\Delta u_v + \Delta d_v)$, $x\Delta u_v$ and $x\Delta d_v$ at $Q_0^2 = 0.5$ GeV^2: dashed — reconstructed from COMPASS data for the first truncated moment of the function $\Delta u_v + \Delta d_v$ at $Q^2 = 10$ GeV^2 [18], solid — original DNS fit [20]. Plots for $x(\Delta u_v + \Delta d_v)$ overlap each other

reconstructed fits and experimental data. The reconstructed combined functions $x(\Delta u_v - \Delta d_v)$ and $x(\Delta u_v + \Delta d_v)$ overlap HERMES and COMPASS results, respectively. For the extracted valence quark densities alone the agreement is worse but still acceptable. We have found, however, that these fits are not unique and an equally good agreement with the data can be obtained with the use of other (not only BB and DNS, respectively) sets of free parameters. When the number of adjustable parameters is large (> 3) and there are no experimental points from the low-x region $x < 0.001$, one cannot distinguish which fit is the best one. Only an additional constraint for small-x behaviour of the parton densities makes the fit procedure more reliable. Let us also mention that due to its large-x sensitivity, the second moment can be helpful in the precise final reconstruction of the parton density [11]. Concluding, even for the large number of adjustable parameters (6 for HERMES and 8 for COMPASS data), the presented method of reconstruction can be a hopeful tool for determining parton densities from experimental results for their truncated moments.

4. TMM IN ANALYSIS OF THE SPIN STRUCTURE FUNCTION g_1

For a complete description of the nucleon spin, one needs two polarized structure functions: g_1 and g_2. Recently, a new generation of experiments with high polarized luminosity performed at the Jefferson Lab allows a more precise study of the polarized structure functions and their moments. This is crucial in our understanding of the QCD spin sum rules, higher-twist effects and quark–hadron duality.

The function g_1 has a simple interpretation in the parton model:

$$g_1(x) = \frac{1}{2} \sum_i e_i \, \Delta q_i(x). \tag{20}$$

Powerful tools to study the internal spin structure of the nucleon are sum rules. One of them is the Bjorken sum rule (BSR) [21], which refers to the first moment of the nonsinglet spin-dependent structure function $g_1^{\mathrm{NS}}(x, Q^2)$:

$$\Gamma_1^{p-n} = \int_0^1 dx \, g_1^{\mathrm{NS}}(x, Q^2) = \int_0^1 dx \, (g_1^p - g_1^n). \tag{21}$$

Due to $SU_f(2)$ flavour symmetry, BSR is regarded as exact. Thus, all of estimations of polarized parton distributions should be performed under the assumption that the BSR is valid. In the limit of the infinite momentum transfer Q^2, BSR has the form

$$\Gamma_1^{p-n} = \int_0^1 dx \, g_1^{\mathrm{NS}}(x, Q^2) = \frac{1}{6} \left| \frac{g_A}{g_V} \right|, \tag{22}$$

where $|g_A/g_V|$ is the neutron β-decay constant

$$\left| \frac{g_A}{g_V} \right| = F + D = 1.28. \tag{23}$$

With the next perturbative orders and higher twists corrections, the BSR reads

$$\Gamma_1^{p-n}(Q^2) = \underbrace{\frac{1}{6}\left|\frac{g_A}{g_V}\right|\left[1-\frac{\alpha_s}{\pi}-3.58\frac{\alpha_s^2}{\pi^2}-20.21\frac{\alpha_s^3}{\pi^3}+\ldots\right]}_{\text{leading twist}} + \underbrace{\sum_{i=2}^{\infty}\frac{\mu_{2i}(Q^2)}{Q^{2i-2}}}_{\text{higher twists}}. \qquad (24)$$

Since experimental data cover only a restricted region of the Bjorken-x variable and, in fact, provide knowledge on truncated moments of the structure functions, it is very natural to use the TMM approach in analysis of these data. The TMM approach allows for a direct study of the contributions to the BSR. In Figs. 3–5 and in the Table, we present the results for the evolution of the first truncated moment of $g_1^{\rm NS}$, namely,

$$\Gamma_1^{p-n}(x_0,1,Q^2) = \int\limits_{x_0}^{1} g_1^{\rm NS}(x,Q^2)\,dx. \qquad (25)$$

Figure 3 shows $\Gamma_1^{p-n}(x_0,1,Q^2)$ as a function of the truncation point x_0 for different scales Q^2. Figure 4 presents the Q^2 evolution of $\Gamma_1^{p-n}(x_0,1,Q^2)$ for different x_0. In Fig. 5

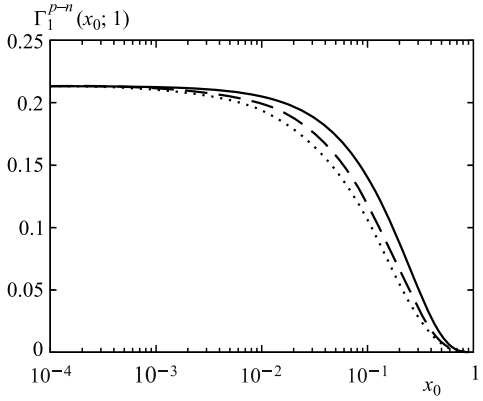

Fig. 3. First truncated moment of g_1^{p-n} vs. truncation point x_0 for different Q^2: 1 GeV^2 (solid), 10 GeV^2 (dashed) and 100 GeV^2 (dotted). We assume Regge input: $g_1^{p-n}(x,Q_0^2) = N(1-x)^3$

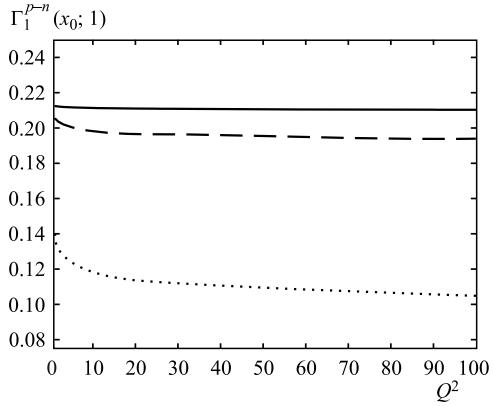

Fig. 4. First truncated moment of g_1^{p-n} vs. evolution scale Q^2 for different truncation points x_0: 0.001 (solid), 0.01 (dashed) and 0.1 (dotted). Regge input parameterization $g_1^{p-n}(x,Q_0^2) = N(1-x)^3$

Theoretical predictions for truncated contributions to the BSR for different small-x behaviour of $g_1^{\rm NS}$. Comparison with the HERMES and COMPASS data

Input	x range	Q^2, GeV^2	$\Gamma_1^{\rm NS}$	EXP $\Gamma_1^{\rm NS}$
$(1-x)^3$			0.161	HERMES
$x^{-0.2}(1-x)^3$	0.021–0.9	5	0.149	$0.1479 \pm 0.0055 \pm 0.0142$
$x^{-0.4}(1-x)^3$			0.131	
$(1-x)^3$			0.177	COMPASS
$x^{-0.2}(1-x)^3$	0.004–0.7	3	0.173	$0.175 \pm 0.009 \pm 0.015$
$x^{-0.4}(1-x)^3$			0.163	

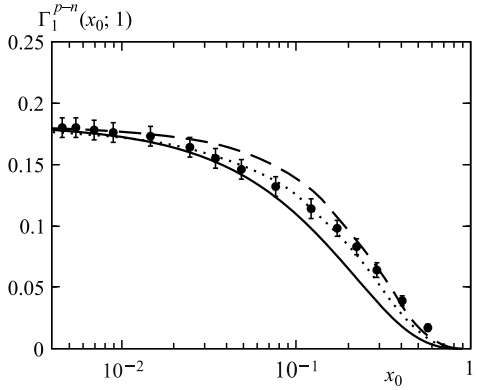

Fig. 5. First truncated moment of g_1^{p-n} vs. truncation point x_0 at evolution scale $Q^2 = 3$ GeV^2 for different small-x behaviour of the input parameterization $g_1^{p-n}(x, Q_0^2) = N\, x^{\alpha}(1-x)^3$: $\alpha = 0$ (solid), -0.2 (dashed) and -0.4 (dotted). Comparison with COMPASS data [22]

we compare our predictions for different input parameterization of the nonsinglet structure function $g_1^{\mathrm{NS}}(x, Q_0^2)$ at the initial scale $Q_0^2 = 1$ GeV^2:

$$g_1^{\mathrm{NS}}(x, Q_0^2) = N x^{\alpha}(1-x)^{\beta}, \tag{26}$$

with experimental COMPASS data [22]. Here, we take into account the first perturbative correction to the BSR: $-\alpha_s/\pi$. In the Table we present truncated contributions to the Bjorken sum rule obtained for different small-x behaviour of the input parameterizations of $g_1^{\mathrm{NS}}(x, Q_0^2)$. Our predictions are compared with experimental HERMES [17] and COMPASS [22] data.

5. TMM IN ANALYSIS OF THE SPIN STRUCTURE FUNCTION g_2

Unlikely g_1, the structure function g_2 has no simple interpretation in the parton model. Due to the technical difficulties of obtaining transversely polarized targets, the structure function g_2 has not been a topic of investigations for a long time. Recently, new experimental data at low- and intermediate-momentum transfers have made g_2 also a valuable and hopeful tool to study the spin structure of the nucleon. The function g_2 provides knowledge on higher-twist effects which are a reflection of the quark–gluon correlations in the nucleon.

The experimental value of the function g_2, measured in the small-to-intermediate Q^2 region, consists of two parts — the twist-2 (leading) and the higher-twist term:

$$g_2(x, Q^2) = g_2^{\mathrm{LT}}(x, Q^2) + g_2^{\mathrm{HT}}(x, Q^2). \tag{27}$$

The leading-twist term g_2^{LT} can be determined from the structure function g_1 via the Wandzura–Wilczek relation [23]:

$$g_2^{\mathrm{LT}}(x, Q^2) = g_2^{\mathrm{WW}}(x, Q^2) = -g_1(x, Q^2) + \int\limits_x^1 \frac{dy}{y}\, g_1(y, Q^2). \tag{28}$$

Then, from the measurements of g_1 and g_2, using the Wandzura–Wilczek approximation, Eq. (28), one is able to extract the higher-twist term g_2^{HT}. In [12], we found a generalization of the Wandzura–Wilczek relation in terms of the truncated moments:

$$\bar{g}_2^n(x_0, Q^2) = \frac{1-n}{n}\, \bar{g}_1^n(x_0, Q^2) - \frac{x_0^n}{n}\, \bar{g}_1^0(x_0, Q^2), \tag{29}$$

where

$$\bar{g}_{1,2}^n(Q^2) = \int_0^1 dx\, x^{n-1}\, g_{1,2}(x, Q^2), \tag{30}$$

$$\bar{g}_{1,2}^n(x_0, Q^2) = \int_{x_0}^1 dx\, x^{n-1}\, g_{1,2}(x, Q^2), \tag{31}$$

and

$$\bar{g}_1^0(x_0, Q^2) = \int_{x_0}^1 \frac{dx}{x}\, g_1(x, Q^2). \tag{32}$$

It is easy to see that for the untruncated moments, Eq. (29) takes the well-known form

$$\bar{g}_2^n(Q^2) = \frac{1-n}{n}\, \bar{g}_1^n(Q^2). \tag{33}$$

From Eq. (29), setting $n = 1$ and $x_0 \to 0$, one can automatically obtain the Burkhardt–Cottingham sum rule (BC) [24] for g_2^{WW}:

$$\int_0^1 dx\, g_2(x, Q^2) = 0. \tag{34}$$

Using the generalization of the Wandzura–Wilczek relation, Eq. (29), for $n = 1$ at two different points of the truncation, and applying the BC sum rule, Eq. (34), we obtain an interesting relation

$$\int_{x_1}^{x_2} dx\, g_2^{\mathrm{WW}}(x, Q^2) = (x_2 - x_1) \int_{x_2}^1 \frac{dx}{x}\, g_1(x, Q^2) - x_1 \int_{x_1}^{x_2} \frac{dx}{x}\, g_1(x, Q^2), \tag{35}$$

which can be very useful in determination of the partial twist-2 contribution to the BC sum rule. Namely, setting $x_1 = 0$ and $x_2 = x_0$, when $x_0 \to 0$, one can get the small-x contribution to the BC sum rule

$$\int_0^{x_0} dx\, g_2^{\mathrm{WW}}(x, Q^2) = x_0 \int_{x_0}^1 \frac{dx}{x}\, g_1(x, Q^2). \tag{36}$$

Now we would like to discuss the problem of the Q^2 evolution of g_2 [12]. While a general DGLAP-type equation for g_2 does not exist, for the twist-3 component of g_2 suitable evolution equation is known (see, e.g., [25]). In the leading twist-2 approximation, the Q^2 evolution

of g_2 is governed by the evolution of g_1, according to the Wandzura–Wilczek relation. Since the second term on the r.h.s. of Eq. (28) is the $n = 0$th truncated moment of the function g_1, Eq. (32), we can rewrite the Wandzura–Wilczek relation in the form

$$g_2^{\mathrm{WW}}(x, Q^2) = -g_1(z, Q^2) + \bar{g}_1^0(z, Q^2) \tag{37}$$

and obtain the evolution equation for g_2^{WW}:

$$\frac{dg_2^{\mathrm{WW}}(x, Q^2)}{d\ln Q^2} = -\frac{dg_1(x, Q^2)}{d\ln Q^2} + \frac{d\bar{g}_1^0(x, Q^2)}{d\ln Q^2}. \tag{38}$$

It is worth noting that according to Eqs. (4) and (5), the $n = 0$th truncated moment of the parton distribution q evolves in the same way as q itself ($P'(0, z) = P(z)$). Taking this into account, in the case of g_1 we obtain from Eqs. (38) and (37) the evolution equation

$$\frac{dg_2^{\mathrm{WW}}(x, Q^2)}{d\ln Q^2} = \frac{\alpha_s(Q^2)}{2\pi} \int\limits_x^1 \frac{dz}{z} P\left(\frac{x}{z}\right) \left[\bar{g}_1^0(z, Q^2) - g_1(z, Q^2)\right], \tag{39}$$

or finally

$$\frac{dg_2^{\mathrm{WW}}(x, Q^2)}{d\ln Q^2} = \frac{\alpha_s(Q^2)}{2\pi} \int\limits_x^1 \frac{dz}{z} P\left(\frac{x}{z}\right) g_2^{\mathrm{WW}}(z, Q^2). \tag{40}$$

The above formula shows that the twist-2 component of the function g_2 obeys the standard DGLAP evolution with the same evolution kernel as g_1. In this way, we obtained a system of evolution equations for

$$g_2 = g_2^{\mathrm{exp}} = g_2^{\mathrm{WW}} + g_2^{\text{twist-3}}, \tag{41}$$

namely,

$$\frac{d\left[g_2^{\mathrm{exp}}(x, Q^2) - g_2^{\mathrm{WW}}(x, Q^2)\right]}{d\ln Q^2} = \\ = \frac{\alpha_s(Q^2)}{2\pi} \int\limits_x^1 \frac{dz}{z} P^{\text{twist-3}}\left(\frac{x}{z}\right) \left[g_2^{\mathrm{exp}}(z, Q^2) - g_2^{\mathrm{WW}}(z, Q^2)\right], \tag{42}$$

$$\frac{dg_2^{\mathrm{WW}}(x, Q^2)}{d\ln Q^2} = \frac{\alpha_s(Q^2)}{2\pi} \int\limits_x^1 \frac{dz}{z} P\left(\frac{x}{z}\right) g_2^{\mathrm{WW}}(z, Q^2). \tag{43}$$

In Figs. 6 and 7, we present numerical solutions of Eq. (40) calculated in LO, for different low-x behaviour of $g_1^{\mathrm{NS}} \sim x^\alpha$ and for different Q^2. Figure 6 shows the predictions for xg_2^{NS} vs. x for different scales of Q^2: 1, 10 and 100 GeV^2. In the input parameterization of $g_1^{\mathrm{NS}} \sim x^\alpha$ we assume at the scale Q_0^2 $\alpha = -0.4$. Note that xg_2^{NS} is positive for low-x, at

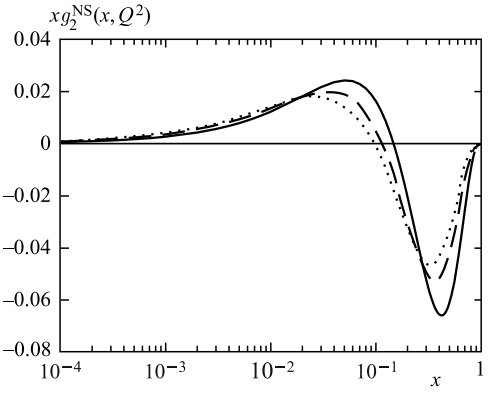

Fig. 6. The nonsinglet LO contributions to the polarized structure function $xg_2^{\rm NS}(x,Q^2)$ as a function of x for different Q^2: 1 GeV^2 (solid), 10 GeV^2 (dashed) and 100 GeV^2 (dotted). Low-x behaviour of $g_1^{\rm NS} \sim x^{-0.4}$

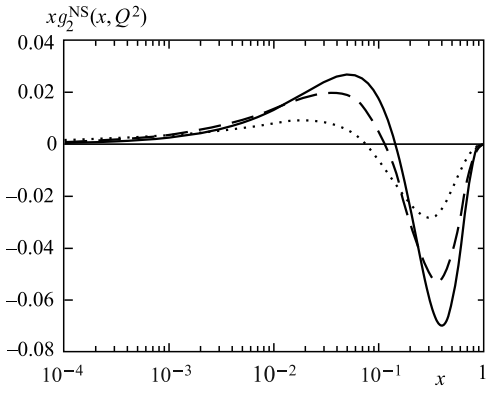

Fig. 7. The nonsinglet LO contributions to the polarized structure function $xg_2^{\rm NS}(x,Q^2)$ at $Q^2 = 10$ GeV^2 vs. x for different low-x behaviour of $g_1^{\rm NS} \sim x^\alpha$: $\alpha = 0$ (solid), $\alpha = -0.4$ (dashed) and $\alpha = -0.8$ (dotted)

about $x = 0.1{-}0.2$ it changes sign and becomes negative for larger x. This is in agreement with the BC sum rule. One can also see that with increasing Q^2, an x-intercept of $g_2^{\rm NS}$ occurs at smaller values of x. In Fig. 7, we compare the predictions for $g_2^{\rm NS}$ for different small-x behaviour of the $g_1^{\rm NS}$ parameterization: $\alpha = 0$, -0.4, -0.8. We find that more singular small-x behaviour of g_1 implies smaller value of the x-intercept of g_2.

6. SUMMARY

This paper is a review of our studies on the truncated Mellin moments of the parton distributions. We presented the evolution equations for the single- and double-truncated nth moments and useful relations between the truncated and untruncated moments. We gave examples of application of our approach to the determination of the PDFs and to QCD analysis of the spin-dependent structure functions g_1 and g_2. We presented the Wandzura–Wilczek relation in terms of the truncated moments, which implies the truncated sum rules. We also discussed the system of the DGLAP evolution equations for g_2. We presented the numerical predictions for the evolution of the truncated moments of $g_1^{\rm NS}$ and the contributions to the BSR. We tested different small-x behaviour of the initial parameterization of $g_1^{\rm NS}$ and compared our results with COMPASS data.

The method of the truncated moments enables one direct, efficient study of the evolution of the moments (and hence sum rules) for nonspin as well as for spin-dependent parton distributions and can be used in all orders of perturbative theory. The adaptation of the evolution equations for the available experimentally x-region provides a new, additional tool for analysis of the nucleon structure functions.

Finally, let us list possible future applications of the TMM approach:

• Study of the fundamental properties of the nucleon structure, concerning moments of F_1, F_2 and g_1. These are: the momentum fraction carried by quarks, quark helicities contributions to the spin of nucleon and, what is particularly important, estimation of the polarized gluon contribution ΔG from COMPASS and RHIC data.

• Determination of Higher-Twist (HT) effects from the moments of g_2 in the restricted x-region, which will be measured at JLab and can provide information on the quark–hadron duality.

• Test of Burkhardt–Cottingham and Efremov–Leader–Teryaev sum rules [26], also for their truncated contributions together with comparison to experimental data.

• Predictions for the generalized parton distributions (GPDs). Moments of the GPDs can be related to the total angular momentum (spin and orbital) carried by various quark flavors. Measurements of DVCS, sensitive to GPDs, will be carried out at JLab. This would be an important step towards a full understanding of the nucleon spin.

Concluding, in light of the recent progress in experimental program, theoretical efforts in improving our knowledge of the nucleon structure functions and their moments are of great importance.

Acknowledgements. DK is grateful to JINR for an opportunity to work here and to BLTP for the warm hospitality.

REFERENCES

1. *Gribov V. N., Lipatov L. N.* Deep Inelastic ep Scattering in Perturbation Theory // Sov. J. Nucl. Phys. 1972. V. 15. P. 438–450.
2. *Gribov V. N., Lipatov L. N.* e^+e^- Pair Annihilation and Deep Inelastic ep Scattering in Perturbation Theory // Ibid. P. 675–684.
3. *Dokshitzer Yu. L.* Calculation of the Structure Functions for Deep Inelastic Scattering and e^+e^- Annihilation by Perturbation Theory in Quantum Chromodynamics // Sov. Phys. JETP. 1977. V. 46. P. 641–653.
4. *Altarelli G., Parisi G.* Asymptotic Freedom in Parton Language // Nucl. Phys. B. 1977. V. 126. P. 298–318.
5. *Forte S., Magnea L.* Truncated Moments of Parton Distributions // Phys. Lett. B. 1999. V. 448. P. 295–302.
6. *Forte S. et al.* Evolution of Truncated Moments of Singlet Parton Distributions // Nucl. Phys. B. 2001. V. 594. P. 46–70.
7. *Piccione A.* Solving the Altarelli–Parisi Equations with Truncated Moments // Phys. Lett. B. 2001. V. 518. P. 207–213.
8. *Forte S. et al.* Determination of α_s from Scaling Violations of Truncated Moments of Structure Functions // Nucl. Phys. B. 2002. V. 643. P. 477–500.
9. *Kotlorz D., Kotlorz A.* Truncated Moments of Nonsinglet Parton Distributions in the Double Logarithmic $\ln^2 x$ Approximation // Acta Phys. Polon. B. 2004. V. 35. P. 705–721.
10. *Kotlorz D., Kotlorz A.* Evolution Equations for Truncated Moments of the Parton Distributions // Phys. Lett. B. 2007. V. 644. P. 284–287.
11. *Kotlorz D., Kotlorz A.* Evolution Equations of the Truncated Moments of the Parton Densities. A Possible Application // Acta Phys. Polon. B. 2009. V. 40. P. 1661–1671.
12. *Kotlorz D., Kotlorz A.* Truncated Mellin Moments: Useful Relations and Implications for the Spin Structure Function g_2 // Acta Phys. Polon. B. 2011. V. 42. P. 1231–1246.
13. *Psaker A. et al.* Quark–Hadron Duality and Truncated Moments of Nucleon Structure Functions // Phys. Rev. C. 2008. V. 78. P. 025206.
14. *Kumano S., Nagai T.-H.* Comparison of Numerical Solutions for Q^2 Evolution Equations // J. Comp. Phys. 2004. V. 201. P. 651–664 and references therein.

15. *El-gendi S. E.* Chebyshev Solution of Differential, Integral and Integro-Differential Equations // Comp. J. 1969. V. 12. P. 282–287.
16. *Kwieciński J., Maul M.* Integral Equation for Spin-Dependent Unintegrated Parton Distributions Incorporating Double $\ln^2(1/x)$ Effects at Low x // Phys. Rev. D. 2003. V. 67. P. 034014.
17. *Airapetian A. et al. (HERMES Collab.).* Precise Determination of the Spin Structure Function g_1 of the Proton, Deuteron and Neutron // Phys. Rev. D. 2007. V. 75. P. 012007.
18. *Alekseev M. et al. (COMPASS Collab.).* The Polarized Valence Quark Distribution from Semi-Inclusive DIS // Phys. Lett. B. 2008. V. 660. P. 458–465.
19. *Blümlein B., Böttcher H.* QCD Analysis of Polarized Deep Inelastic Data and Parton Distributions // Nucl. Phys. B. 2002. V. 636. P. 225–263.
20. *de Florian D., Navarro G. A., Sassot R.* Sea Quark and Gluon Polarization in the Nucleon at NLO Accuracy // Phys. Rev. D. 2005. V. 71. P. 094018.
21. *Bjorken J. D.* Asymptotic Sum Rules at Infinite Momentum // Phys. Rev. 1969. V. 179. P. 1547–1553.
22. *Alekseev M. et al. (COMPASS Collab.).* The Spin-Dependent Structure Function of the Proton g_1^p and a Test of the Bjorken Sum Rule // Phys. Lett. B. 2010. V. 690. P. 466–472.
23. *Wandzura S., Wilczek F.* Sum Rules for Spin-Dependent Electroproduction: Test of Relativistic Constituent Quarks // Phys. Lett. B. 1977. V. 72. P. 195–198.
24. *Burkhardt H., Cottingham W. N.* Sum Rules for Forward Virtual Compton Scattering // Ann. Phys. 1970. V. 56. P. 453–463.
25. *Geyer B., Mueller D., Robaschik D.* Evolution Kernels of Twist-3 Light-Ray Operators in Polarized Deep Inelastic Scattering // Nucl. Phys. B. Proc. Suppl. 1996. V. 51. P. 106–110.
26. *Efremov A. V., Teryaev O. V., Leader E.* An Exact Sum Rule for Transversely Polarized DIS // Phys. Rev. D. 1997. V. 55. P. 4307–4314.

Received on October 31, 2013.